J Wood Sci (2004) 50:41–46
DOI 10.1007/s10086-003-0524-z

ORIGINAL ARTICLE

Mats Ekevad

Method to compute fiber directions in wood from computed tomography images

Received: July 26, 2002 / Accepted: February 10, 2003

Abstract This paper describes a new method, called the CT-direction method, in which the fiber directions in wood in three-dimensional space are calculated from the pixel information on a series of two-dimensional computed tomography images. Local fiber directions are calculated from the principal directions of inertia of measurement spheres distributed throughout the body of the wood object. The calculated fiber directions are probably due to density streaks in the material, such as fiber bundles, which are directed in the fiber direction, and not the density of individual fibers, which are too small to be detected. The fiber directions vary locally, and density streaks from knots, growth rings, and compression wood influence the results, which adds spread to the results. The fiber directions are presented as spiral grain angles and conical angles and are compared with spiral grain angles measured with the tracheid-effect method. The comparisons show that the CT-direction method is a nondestructive way to measure fiber directions locally and in the interior of the body of a piece of wood.

Key words Wood · Fiber direction · Spiral grain · Computed tomography · FEM

Introduction

Computed tomographic (CT) images of the interior of a piece of wood are often easy to understand, as the example in Fig. 1 shows. The pith position, growth rings, knots, areas with compression wood, and juvenile wood can be visually observed as characteristic patterns, streaks, points, lines, or areas in the image. A CT image is a matrix of discrete density values, called pixel values, viewed as a two-dimensional (2-D) contour plot. The CT scanning process produces a three-dimensional (3-D) description of the density as a series of images with the wood object being translated a bit between each image. The geometric resolution of the image is the pixel size (i.e., the size of the volume for which each discrete density value stands). The pixel values for the series of 2-D images are stored on data files and can be handled with computer programs.

The pith position and the tangential and radial directions of the growth rings can be determined visually from a 2-D CT image of a section perpendicular to the pith direction. However, the fiber directions, which are approximately along the pith direction, are not directly visible. The CT-direction method described in this paper calculates local fiber directions in the body of a wood object from the information in a series of 2-D CT images.

One use for the local fiber directions is for finite element (FE) calculations on wood, for which an orthotropic material model is used. Knowledge of the orthotropic stiffnesses (i.e., the elastic moduli) in the material is required as well as the orthotropic directions themselves (i.e., radial, tangential, and fiber directions). The CT-direction method suggests a new way to achieve local, orthotropic directions for wood to be used for FE calculations. If such local data are used in FE calculations, realistic simulations of drying deformations of real planks are possible; and local crooks, twists, and bows can be simulated.

No other methods to detect 3-D fiber directions automatically in a computer program from CT images are known to the author, although Sepulveda[1] manually measured the spiral grain angle from CT images of a log by creating images on concentric surfaces and recognizing patterns in the images. Investigations of other phenomena in the 3-D interior of wood by CT have also been reported. Bhandarkar et al.[2] used CT to detect internal log defects and to determine how they are directed. Illman and Dowd[3] used 3-D microtomography to obtain spatial information and characterize the structural integrity of wood. Values for the spiral grain angle and older, traditional methods for measuring the spiral grain angle have been reported by Harris.[4]

M. Ekevad (✉)
Division of Wood Technology, Skellefteå Campus, Luleå University of Technology, Skeria 3, S-931 87 Skellefteå, Sweden
Tel. +46-910-585377; Fax +46-910-585399
e-mail: mats.ekevad@tt.luth.se

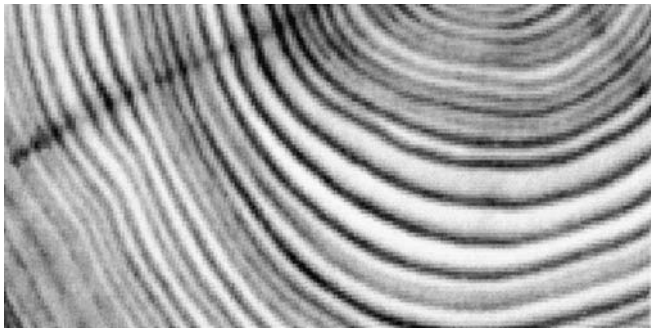

Fig. 1. Two dimensional computed tomography (2-D CT) image of a section through a piece of wood. The densities are in the range of 235 kg/m^3 (*white areas*) to 557 kg/m^3 (*black areas*). Plank E, section 22

Theory

Principal directions

The radial, tangential, and fiber directions are calculated from the principal moments of inertia and the principal directions of fictitious, small (4–15 mm diameter) "measurement bodies" (spheres) that are distributed throughout the inside the body of the piece of wood. The theory is as follows: The mass center position X_{cg}, Y_{cg}, Z_{cg} of a specific body is

$$X_{cg} = \frac{\int_V X\rho dV}{\int_V \rho dV}, \quad Y_{cg} = \frac{\int_V Y\rho dV}{\int_V \rho dV}, \quad Z_{cg} = \frac{\int_V Z\rho dV}{\int_V \rho dV} \tag{1}$$

where ρ is the density, V is the volume of the body, and X-Y-Z is an arbitrarily placed Cartesian coordinate system. The integrations are performed numerically with the density distribution known at discrete points and interpolated values in between. The mass distribution of the body is described by the moment of inertia tensor

$$\bar{I} = \begin{bmatrix} I_{xx} & -I_{xy} & -I_{xz} \\ -I_{xy} & I_{yy} & -I_{yz} \\ -I_{xz} & -I_{yz} & I_{zz} \end{bmatrix} \tag{2}$$

where

$$I_{xx} = \int_V \left(y^2 + z^2\right)\rho dV, \quad I_{xy} = \int_V xy\rho dV, \quad I_{xz} = \int_V xz\rho dV,$$
$$I_{yy} = \int_V \left(x^2 + z^2\right)\rho dV, \quad I_{yz} = \int_V yz\rho dV, \quad I_{zz} = \int_V \left(x^2 + y^2\right)\rho dV \tag{3}$$

and x-y-z is a Cartesian coordinate system that has its origin in the mass center of the body. The principal directions (eigenvectors) and principal values (eigenvalues) for $\bar{I}$ are calculated as the solutions of the eigenvalue problem

$$\left(\bar{I} - \bar{\lambda}\,\bar{E}\right)\bar{P} = \bar{0} \tag{4}$$

where $\bar{\lambda}$ is a diagonal matrix containing the three principal values on the diagonal, $\bar{E}$ is the identity matrix, and $\bar{P}$ is a matrix with the three principal directions as column vectors. The principal values are the principal moments of inertia, and the principal directions are the principal directions of inertia.

The three principal moments of inertia are, in general, unequal for a spherical body with an arbitrarily varying mass distribution; as a result, the three principal directions are unique and orthogonal. There are interesting special cases, however, such as the double and triple eigenvalue problem. For a spherical body the geometry in itself does not prefer any direction; consequently, a spherical body with constant density has arbitrarily directed principal directions, and all three principal moments of inertia are equal. In this case we have a triple eigenvalue problem, and the column vectors in $\bar{P}$ are three arbitrary but orthogonal directions.

In the case of two principal moments of inertia being equal we have a double eigenvalue problem, and the principal directions belonging to the double eigenvalues are arbitrarily directed in a specific plane. Thus, $\bar{P}$ contains two arbitrary but orthogonal vectors in the specific plane and one unique column vector normal to the specific plane. Two special cases for wood exemplify the double eigenvalue problems: For a spherical body containing a plane slice or layer of material with a density different from the rest of the body, such as a growth ring layer, the unique principal direction lies in the direction normal to the layer, and the other two directions lie arbitrarily in the plane of the layer. For a spherical body containing a small straight cylinder of material with a density different from the rest of the body, such as a fiber bundle, one principal direction lies in the direction of the small cylinder, and the other two directions lie arbitrarily directed in the plane perpendicular to the first principal direction.

The question of whether a principal direction is unique is, in practice, treated in the following way. The ratios between the eigenvalue in question and the two other eigenvalues are formed; if they differ from 1 by more than ε, the eigenvalue in question is unique. The ε value is a nondimensional limit defined by the user.

The primary cause of unique principal directions in wood is the growth rings (i.e., density variations in the radial direction). A growth ring is approximately a conical layer in the material that consists of an inner sublayer of earlywood with low density and an outer sublayer of latewood with high density. Growth rings from consecutive years appear in a piece of wood as a series of concentric conical layers. An eigenvalue calculation for a sphere containing such layered material results in three eigenvectors approximately in the radial, tangential, and axial directions of the cone and three corresponding eigenvalues. The tangential and axial eigenvalues may be equal or nearly equal, which indicates that the unique direction is the radial direction and that all vectors lying in the plane spanned by the tangential and axial eigenvectors are eigenvectors. However, if streaks of material with a density different from that of the surrounding material exist and point in the fiber

direction, the axial eigenvector is unique and points in the fiber direction.

There is a need for a statistical averaging procedure when calculating fiber directions because not only fiber bundles influence the density distribution; knots, compression wood, ray cells, and noncircular or markedly curved growth rings affect the calculated directions. Results for individual spheres vary, and it is necessary to take an average over a number of spheres to obtain meaningful results. The pixel size also influences the results and sets a limit for how small the material streaks which are possible to detect may be. The sphere size sets a limit for how large the material streaks (also possible to detect) may be.

For FE purposes it is, in addition to knowing the orthotropic stiffnesses, necessary to know the local material directions; the pith position and spiral grain angle are not interesting in themselves. However, it is interesting to calculate traditional measures such as the spiral grain angle to compare results from the CT-direction method with the results of other methods.

Calculation of fiber angles

The series of 2-D CT images are put in an *X-Y-Z* Cartesian coordinate system. The *X-Y* coordinate plane is parallel to the image planes, and *Z* is the axial coordinate, directed perpendicular to the image planes, approximately along the pith direction. At first the pith positions for all sections are either determined by visual inspection of the images or are calculated by an other method. Here the pith positions are calculated automatically by a method suggested by Ekevad (to be published). The succession of pith positions is a curve in 3-D space, called the pith curve. Approximate radial, tangential, and axial directions are calculated for each sphere from the pith position and the position of the sphere center.

Eigenvectors for all spheres are calculated and sorted in the order radial, tangential, and axial eigenvectors by comparing the eigenvectors with the approximate radial, tangential, and axial directions. The axial eigenvector is assumed to point in the fiber direction and is called $\overline{\psi}$.

The spiral grain angle β and the conical angle φ are calculated by projecting $\overline{\psi}$ on two planes. The first is the tangential plane to the growth ring cone through the point in question, and the second is the pith plane, which is spanned by the pith direction vector $\overline{m}$ and the radius vector $\bar{r}$, (Fig. 2). The calculations for a sphere with its center point position vector $\bar{x} = (X_{cg}, Y_{cg}, Z_{cg})^T$ are as follows, where $\overline{x_0}$ is the pith position vector for the section which is closest to the sphere's center point, and $\overline{m}$ is the pith direction vector (directed from the pith position in the current section to the pith position in the next section). The radial vector

$$\bar{r} = \bar{x} - \overline{x_0} - \left[\overline{m} \cdot \left(\bar{x} - \overline{x_0}\right)\right]\overline{m} \tag{5}$$

is the shortest possible vector from the pith curve to the sphere center. The pith plane spanned by $\bar{r}$ and $\overline{m}$ has the normal vector

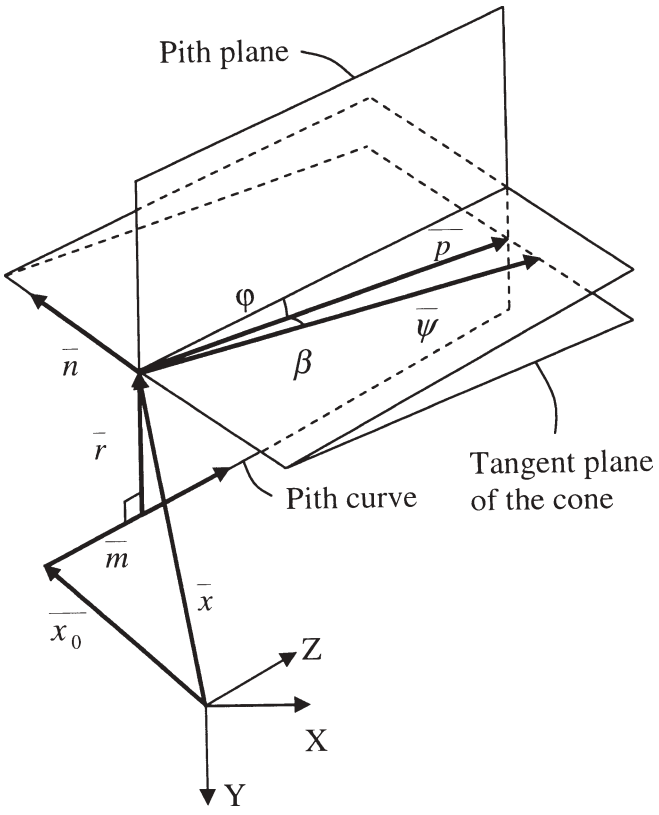

Fig. 2. Geometry in three-dimensional space. The spiral grain angle β and the conical angle φ for a sphere with center point position vector $\bar{x}$. The pith position vector is $\overline{x_0}$, and the pith direction vector is $\overline{m}$. The radius vector is $\bar{r}$, and $\overline{n}$ is the normal vector of the pith plane. The eigenvector in the fiber direction is $\overline{\psi}$, and its projection on the pith plane is $\overline{p}$

$$\overline{n} = \frac{\bar{r} \times \overline{m}}{\left|\bar{r} \times \overline{m}\right|} \tag{6}$$

and

$$\overline{p} = \overline{n} \times \left(\overline{\psi} \times \overline{n}\right) \tag{7}$$

is the projection of the eigenvector in the fiber direction $\overline{\psi}$ on the pith plane. The conical angle φ where

$$|\varphi| = \arccos\left(\overline{p} \cdot \overline{m}\right) \tag{8}$$

is the angle between $\overline{m}$ and $\overline{p}$. The sign of φ is defined to be positive if

$$\bar{r} \cdot \overline{p} < 0 \tag{9}$$

which means a decreasing growth ring radius with increasing axial coordinate, and negative otherwise. Normally, φ is positive if the positive axial coordinate direction is from the root to the top of the tree. The tangent plane of the cone in the actual point $\bar{x}$ is spanned by $\overline{p}$ and $\overline{\psi}$. The spiral grain angle β, where

$$|\beta| = \arccos\left(\overline{\psi} \cdot \overline{p}\right) \tag{10}$$

is the angle between $\overline{\psi}$ and $\overline{p}$. The sign of β is positive if

$$\overline{\psi} \cdot \overline{n} < 0 \tag{11}$$

which means that a positive twist is right-handed, as in a right-hand threaded screw. Normally, β is negative in the wood objects treated here (i.e., left-handed spiral grain).

Materials, methods, results

The CT images of two planks of Norway spruce (*Picea abies*) from northern Sweden, designated planks D and E with cross sections measuring 85 × 40 mm and lengths 350 mm were analyzed according to the above procedure. The planks were free from knots in the areas treated but achieved a twist deformation of about 4 degrees/m during the drying process, which indicates that the spiral grain angles were rather large. The distances between the CT images were 2 mm, and the centers of the spheres were evenly distributed over each image area with 1 mm distance between adjacent sphere centers for both planks. The fiber directions β and φ were calculated and are shown in Figs. 3–6 for one axial position in plank D and two axial positions in plank E. Spheres with centers in three to five images were used to calculate the fiber directions for each axial position. Unique eigenvectors in the fiber direction were ensured by setting ε at 0.005 for plank D and at 0.004 for plank E, values that have been used to give low spread in the final results. Sphere diameters were 7 mm for plank D and 4 mm for plank E; the pixel size was 0.4466 mm; and the distances between growth rings were in the range of 1.5–5.0 mm.

The results for β are presented in two alternative ways for plank D in Fig. 3 and for the two axial positions for plank E in Figs. 5 and 6. The first way to present the results is as all but a few of the individual β-values for all the spheres which fulfil the condition for uniqueness of the eigenvector (a few β-values are outside the limits of the diagrams and are not shown). The second way to present the results is as statistical measures for groups of β-values. Here mean-, mid-, lower quartile- and upper quartile-values for β are shown for all spheres which lie in groups with radii 0–10, 10–20 mm and so on. The φ value is shown in Fig. 4 for plank D and only as individual values for each sphere. The angles φ and β are presented as functions of the radius to the pith (i.e., the distance from the sphere center of gravity to the pith).

Measured values of the angle β with the method developed by Nyström[5] are shown in Figs. 3, 5, and 6 for comparison. These values are measured at a single point on the plank upper side for each radius. The chosen points for measurement are "good" points; that is, no knots or other phenomena are visible near the points.

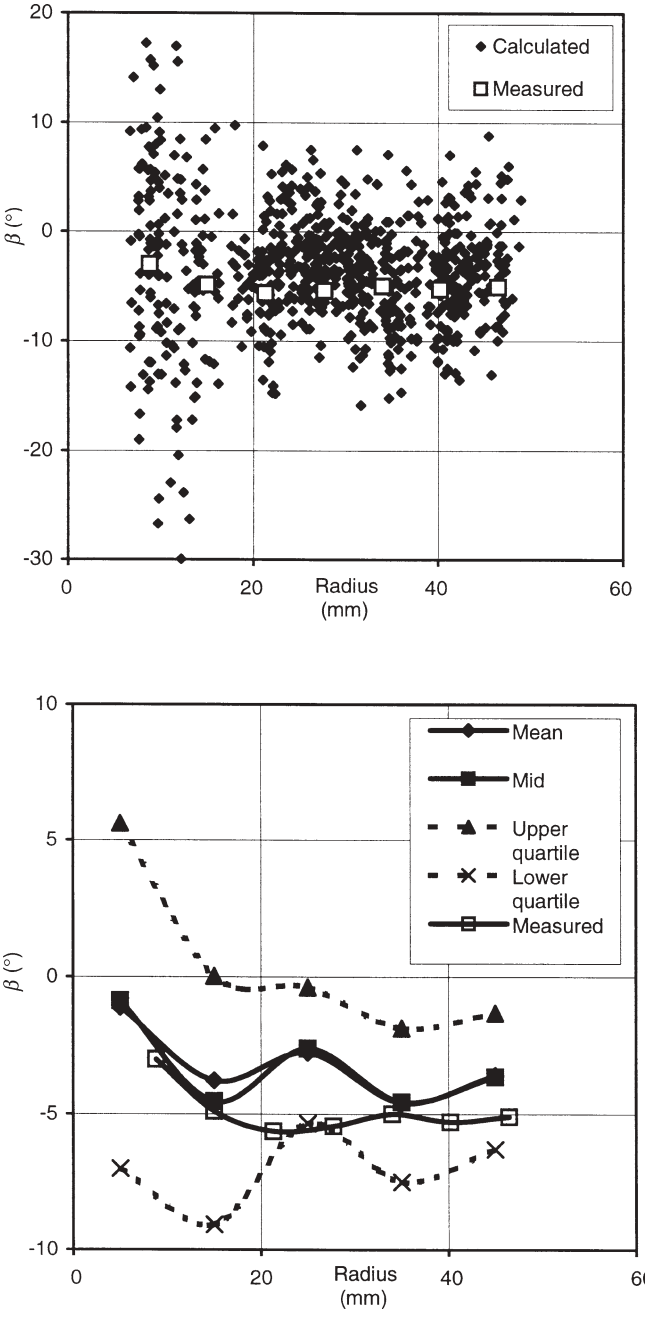

Fig. 3. Calculated spiral grain angle β for the spheres in sections 3–7 in plank D as a function of the radius from the pith. The factor ε is 0.005, which gives 792 unique angles from a total of 9990 spheres. Spiral grain angle β was measured by the tracheid-effect method by Nyström.[5] The mean, mid, lower quartile, and upper quartile values for the data were collected from five groups with radii of 0–10, 10–20, 20–30, 30–40, and 40–50 mm

Discussion

Figures 3, 5, and 6 show the variation in spiral grain angles between the individual spheres in the three test cases. There is significant spread in the results for individual spheres, and a possible explanation is as follows: The CT-direction method detects directions in the density distribution in the piece of wood, directions that are due to systematic density variations. The pixel size used here is not small enough to capture density variations between individual fibers; it probably captures density variations due to bundles of fibers and other density streaks that follow the fiber direction. However, the density variations, which reveal the fiber directions, are not particularly significant compared to

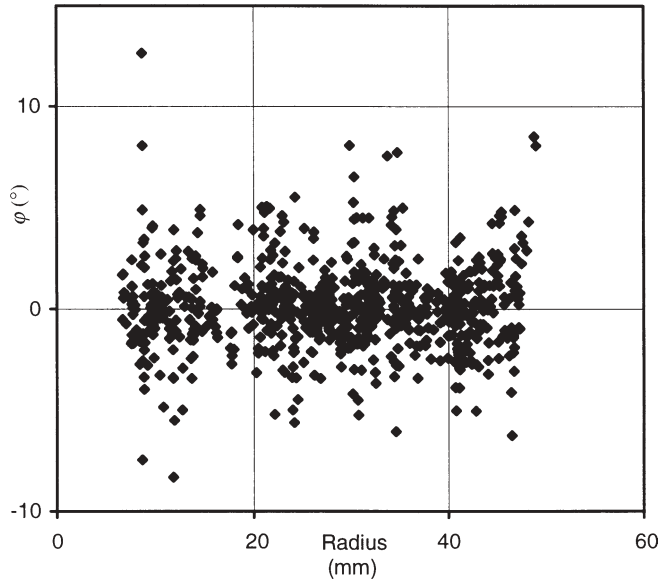

Fig. 4. Conical angle φ for the same spheres as in Fig. 3 as a function of the radius from the pith

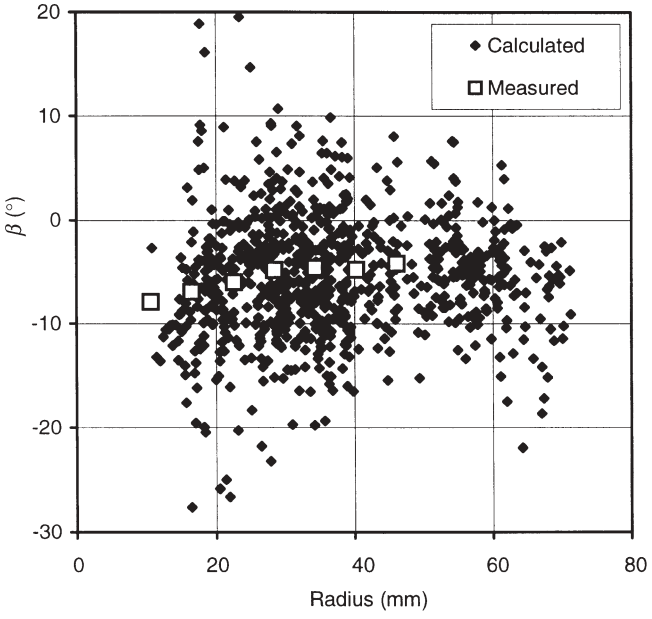

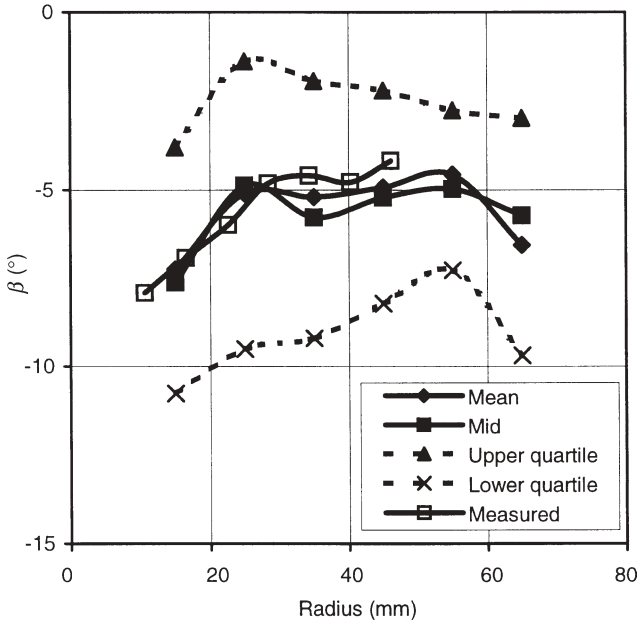

Fig. 5. Calculated spiral grain angle β for the spheres in sections 10–12 in plank E as a function of the radius from the pith. The factor ε is 0.004, which gives 858 unique angles from a total of 8160 spheres. Spiral grain angle β was measured by the tracheid-effect method by Nyström.[5] The mean, mid, lower quartile, and upper quartile values for the data were collected from six groups with radii of 10–20, 20–30, 30–40, 40–50, 50–60, and 60–70 mm

other causes of density variations, such as knots, growth rings, and compression wood. Therefore, the calculations of spiral grain angles and conical angles have a significant spread, and statistical treatment of the results from many individual spheres is needed.

The mean and mid values in Figs. 3, 5, and 6 agree well with the results from the tracheid-effect method of Nyström.[5] The spiral grain angles are rather large (about 5 degrees left-handed), as would be expected from the large twists of the planks that occur during the drying process. The conical angle φ is about 0 degrees/m (Fig. 4), a value that seems reasonable for the short (<10 cm) axial lengths studied, although no other data are available for comparison.

It is found, in general, that the spread decreases if spheres from more than one image are combined because the increased number of spheres gives a more reliable statistical evaluation. However, the spreads are increased if more than about three to five images are grouped together which indicate that the fiber directions (or the possibility of detecting fiber directions), vary in the axial direction of the planks. Also, certain images give more spread than others: compare Figs. 3 and 6, which indicate that certain sections of the planks contain fewer or smaller fiber bundles, which are more difficult to detect than those in other sections. The spread is generally larger for small radii than for large radii (Figs. 3, 5). Part of that spread is due to the fact that small errors in the pith position or in the fiber angles influence the calculation of spiral grain angles for small radii more than for large radii.

The figures describe the angles β and φ as functions of the radial coordinates, as they are usually described. Generally, however, there are also variations in the tangential direction, in the axial direction, and around knots, which cause part of the spreads in the figures.

The sphere size and the pixel size determine the size of the density streaks, which are possible to detect. Decreased sizes make it possible to detect smaller density streaks. The sphere sizes used here, 4 and 7 mm, were used to give as small a spread as possible, and they worked about equally well for planks D and E. The pixel size used was as small as possible with the available CT scanner.

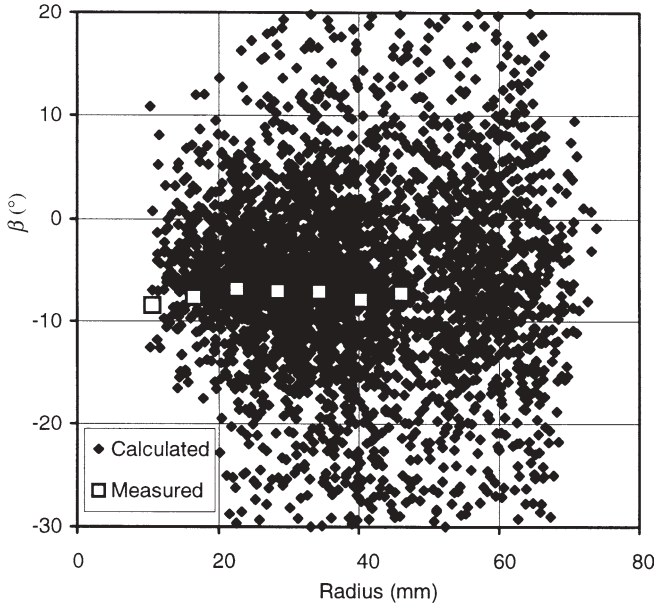

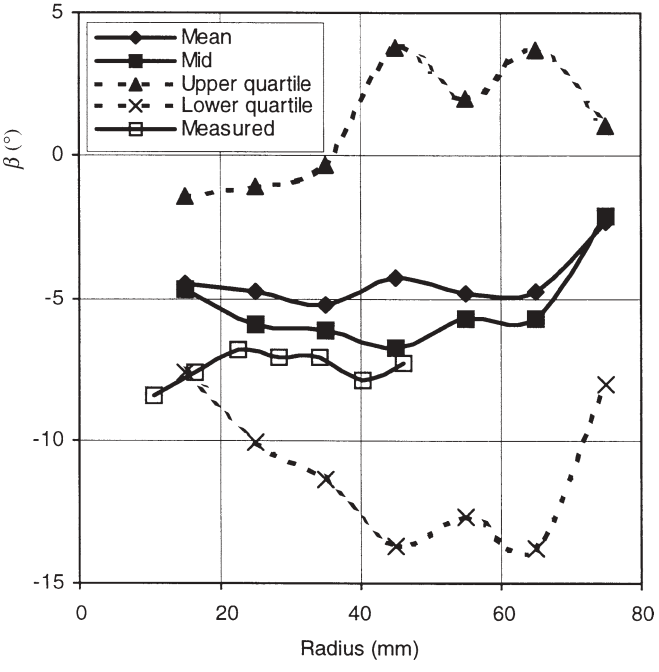

Fig. 6. Calculated spiral grain angle β for the spheres in sections 20–24 in plank E as a function of the radius from the pith. The factor ε is 0.004, which gives 2414 unique angles from a total of 13600 spheres. Spiral grain angle β was measured by the tracheid-effect method by Nyström.[5] The mean, mid, lower quartile, and upper quartile values for the data were collected from seven groups with radii of 10–20, 20–30, 30–40, 40–50, 50–60, 60–70, and 70–80 mm

Conclusions

The results presented in this paper show that the axial eigenvector, if it is unique, points in the fiber direction in an average sense. Thus, the CT-direction method works and can be used to detect local fiber directions for various purposes (e.g., for FE calculations). It is also possible to use the method to obtain 3-D density data, which are measured with methods other than CT. Further work, such as investigations of the influence of the pixel size of the tomograph, could improve the CT-direction method.

Acknowledgment I thank Formas (the Swedish Research Council for Environment, Agricultural Sciences and Spatial Planning) for their support.

References

1. Sepulveda P (2000) Non-destructive measurement of spiral grain with computed tomography. Licentiate thesis, Luleå University of Technology, Division of Wood Technology, Skellefteå, Sweden
2. Bhandarkar SM, Faust TD, Tang M (1999) Catalog: a system for detection and rendering of internal log defects using computer tomography. Machine Vis Applications 11:171–190. Springer-Verlag, Berlin Heidelberg
3. Illman B, Dowd B (1999) High-resolution microtomography for density and spatial information about wood structures. In: Proceedings of SPIE – The International Society for Optical Engineering, v3772; Proceedings of the 1999 developments in X-ray tomography II, Denver, pp 198–204
4. Harris JM (1989) Spiral grain and wave phenomena in wood formation. Springer-Verlag, Berlin Heidelberg
5. Nyström J (2000) Automatic measurement of fiber orientation in softwoods by using the tracheid effect. In: Kline DE, Abbott AL (eds) Proceedings of the fourth international conference on image processing and scanning of wood, Mountain Lake, VA

The publication of this article was made possible by an Emachu Research Fund. The author is grateful for the fund.